Supporting Information

High sensing performance flexible nanocomposite sensor with a hybrid nanostructure constructed via nanoscale confined motion of nanofibers and nanoplatelets

Zhenghui Xie[1,2], Feiran Meng[1], Junlong Yang[1], Yuhong Wang[3], Chul B. Park[1,4], Pengjian Gong[1*] and Guangxian Li[1]

1. *College of Polymer Science and Engineering, State Key Laboratory of Polymer Materials Engineering, Sichuan University, 24 Yihuan Road, Nanyiduan, Chengdu, Sichuan, People's Republic of China, 610065*
2. *Jiangsu JITRI Advanced Polymer Materials Research Institute, Tengfei Building, 88 Jiangmiao Road, Jiangbei New District, Nanjing, Jiangsu, People's Republic of China, 211800*
3. *Chinese Academy of Sciences, Chengdu Institute of Organic Chemistry, 519 Luxikou North Road, Xinglong Street, Tianfu New Area Chengdu, Sichuan, People's Republic of China, 610213*
4. *Microcellular Plastics Manufacturing Laboratory, Department of Mechanical and Industrial Engineering, University of Toronto, 5 King's College Road, Toronto, Ontario, Canada, M5S 3G8*

* Corresponding Author: Pengjian Gong. Email address: pgong@scu.edu.cn. Tel: +86 (028) 8540-1841

The nanoparticle content in nanocomposite was fixed at 15 wt%. The nanoparticle was mixed with thermoplastic polyurethane (TPU) matrix by solution blending at various proportions of carbon nanofiber (CNF) and graphene nanoplatelet (GNP) as shown in Figure S1. The nanocomposite was then foamed by supercritical CO_2 ($scCO_2$) to prepare CNF/GNP/TPU nanocomposite foam.

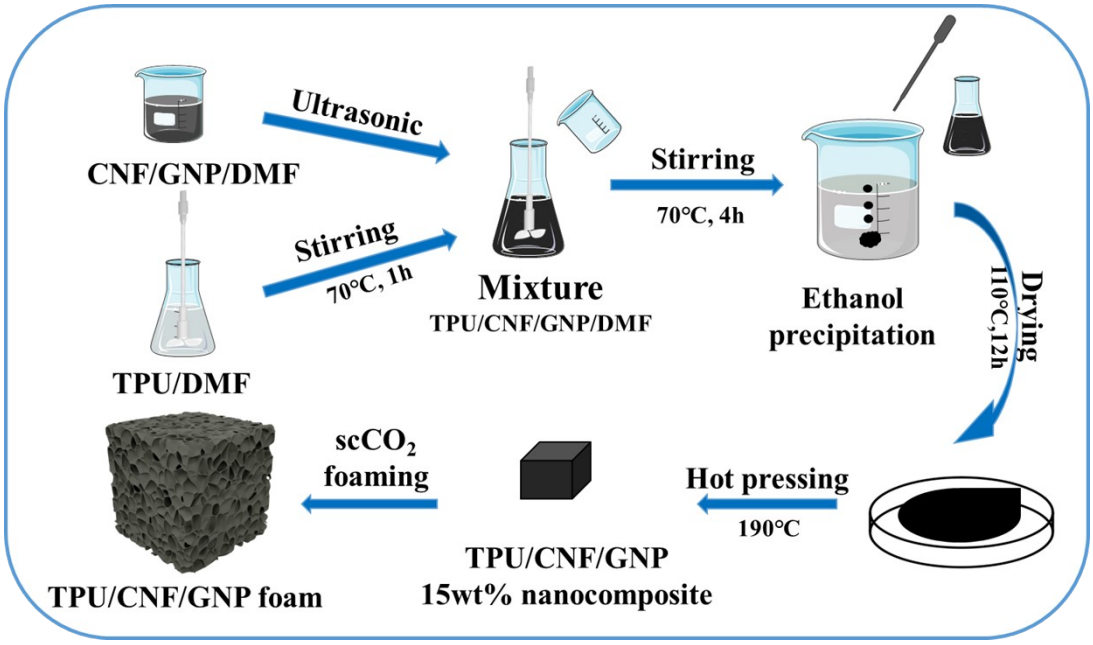

Figure S1 Sample preparation process

CNF/TPU (sample 1D), GNP/TPU (sample 2D) and CNF/GNP/TPU nanocomposites (samples of 1D/2D 4:1, 1D/2D 2:1, 1D/2D 1:1 and 1D/2D 1:2) were all foamed by $scCO_2$ at various foaming temperatures (145°C, 150°C, 155°C and 160°C) and the corresponding foam morphology was summarized in Figure S2. Foam expansion ratio (ER) was calculated using formula S1.

$$ER = \frac{\rho_{solid}}{\rho_{foam}} \quad (S1)$$

where ρ_{solid} is the density of solid sample before foaming and ρ_{foam} is the density of foam sample.

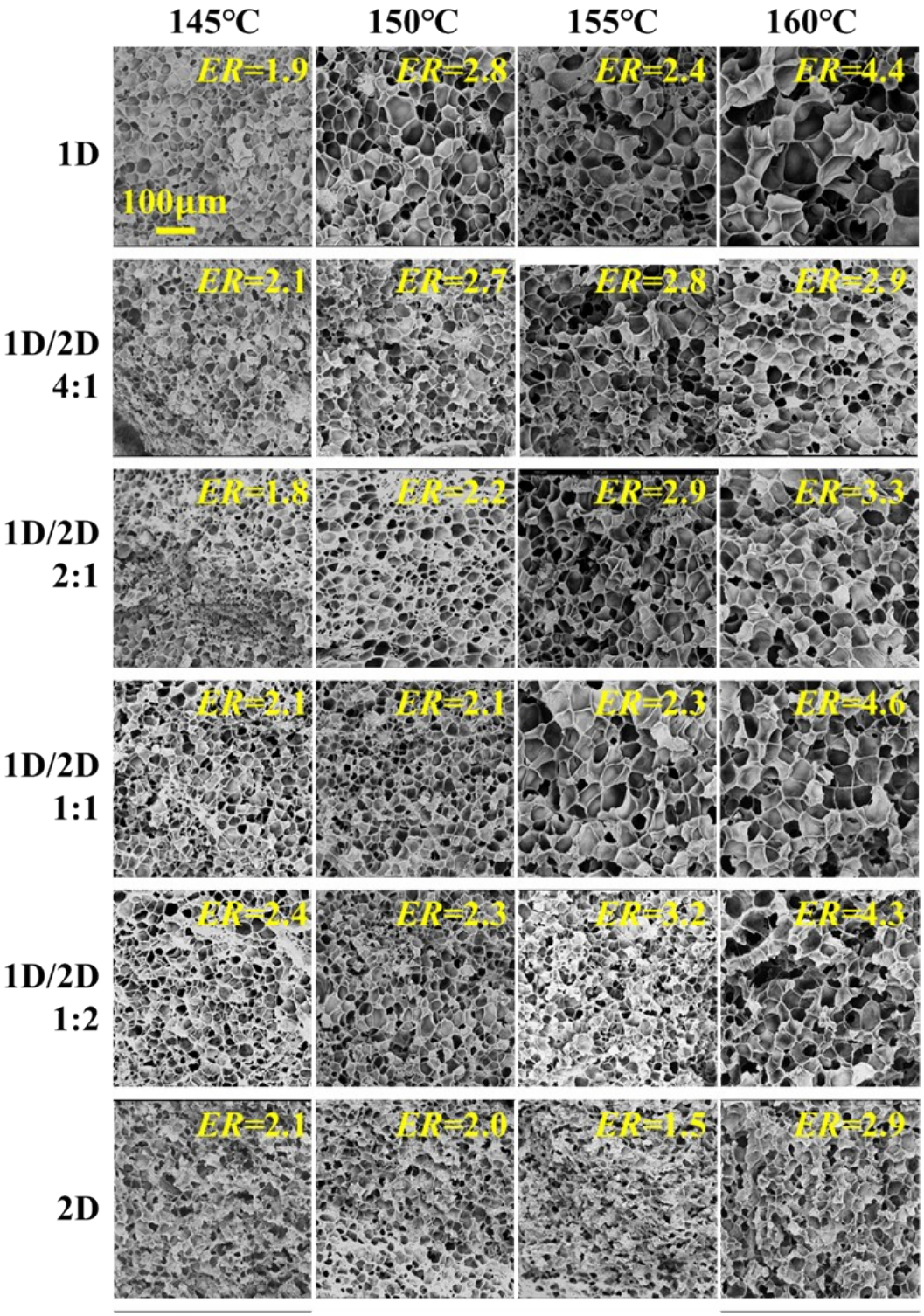

Figure S2 SEM micrographs of nanocomposite foams (samples 1D, 1D/2D 4:1, 1D/2D 2:1, 1D/2D 1:1, 1D/2D 1:2, 2D) at various foaming temperatures (145°C, 150°C, 155°C and 160°C) together with sample expansion ratio

Image-J Pro software was used to analyze the above SEM micrographs to obtain

the statistical average cell diameter (D) and to calculate the cell density (N_f) using formula S2.

$$N_f = \left(\frac{N}{A}\right)^{3/2} \times ER \qquad (S2)$$

where N is the number of cells in SEM micrographs and A is the area of the actual analyzed place in SEM micrographs (cm^2).

Figure S3 shows the statistical cell size and cell density of nanocomposite foams. It can be seen that when the foaming temperature is low, the cell diameter is small and the cell density is low. With the increase of foaming temperature, the matrix strength decreases and it becomes more conducive to cell growth. Therefore, the cell size increases at a higher foaming temperature.

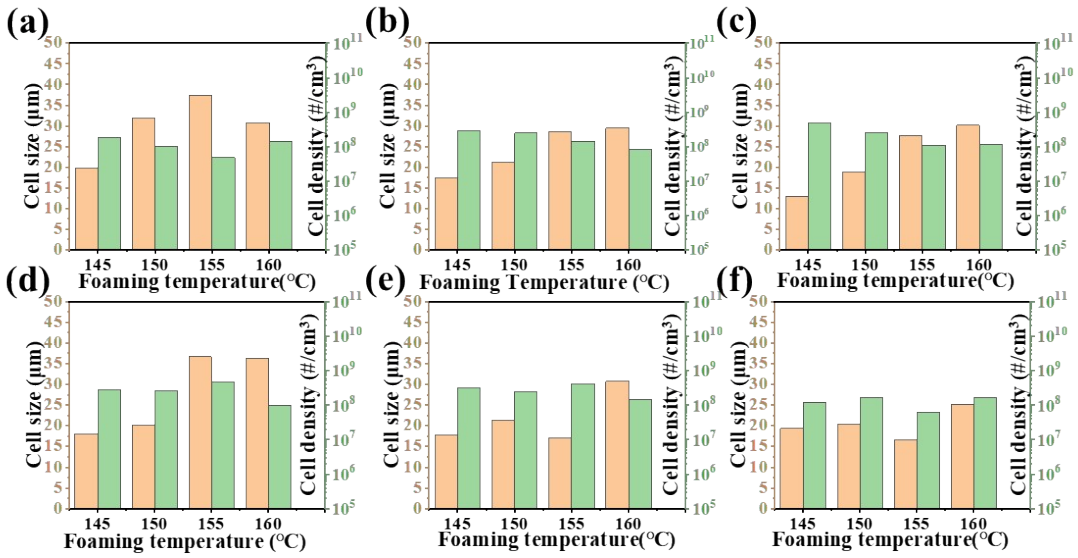

Figure S3 Cell size (▭) and cell density (▭) of nanocomposite foams: (a) sample 1D, (b) 1D/2D 4:1, (c) 1D/2D 2:1 (d) 1D/2D 4:1, (e) 1D/2D 4:1, (f) sample 2D

An effective conductive network can be constructed within the matrix by increasing nanoparticle content. According to the experimental conductivity curves in Figure S4, 1D CNF/TPU nanocomposite has good conductivity at a low nanoparticle content, but its percolation area is narrow. As for 2D GNP/TPU nanocomposite, a high content of nanoparticle is required to construct the conductive network. For the

nanocomposite with hybrid 1D CNF/2D GNP nanoparticles, a proper nanoparticle content is enough to construct the conductive network and a broad percolation area is observed in the electrical conductivity curve. According to this result, the content of the nanoparticle at the percolation point can make the hybrid nanocomposite foam with a high sensing response, so we choose the ratio of 15 wt% as an optimal nanoparticle content.

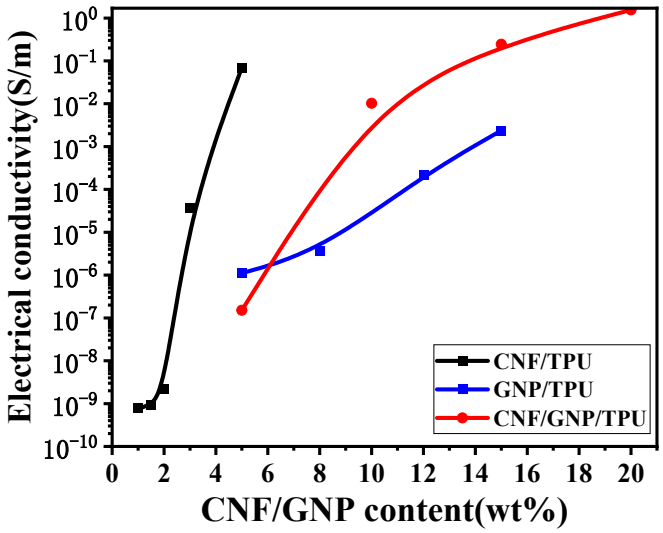

Figure S4 Electrical conductivity of 1D CNF/TPU, 2D GNP/TPU and 1D CNF/2D GNP/TPU (1D/2D 2:1) nanocomposites as a function of nanoparticle content

The volume fraction of CNFs and GNPs is directly related to the expansion ratio of nanocomposite foams. The mass fraction of CNFs and GNPs is then converted into volume fraction using formula S3:

$$Vol_{particles} = \frac{m_{particles}}{ER \times \rho_{particles} \times V_0} \quad \text{(S3)}$$

where $\rho_{particles}$ is the density of the carbonaceous nanoparticles, $m_{particles}$ is the mass of carbonaceous nanoparticles in nanocomposite, V_0 is the volume of the unfoamed nanocomposite.

By adding 12 vol% nanoparticle into TPU, the nanocomposites show good

electrical conductivity behavior. Because CNF with 1D characteristic is more easily contacted with adjacent carbonaceous nanoparticle to form a conductive network than GNP with 2D characteristic, the electrical conductivity of hybrid nanocomposites gradually decreased with increasing GNP proportion while keeping a constant total nanoparticle content, as shown in Figure S5. When nanocomposites were foamed by $scCO_2$, the introduction of air would decrease the volume content of nanoparticles, and hence decrease the conductivity to varying degree depending on the air content. The conductivity of foam samples after foaming at various temperatures were summarized in Figure S5 as well. It is noted that despite the large air volume in nanocomposite after $scCO_2$ foaming, foam samples of 1D (only CNF) and 1D/2D 4:1 still have high conductivity due to the large amount of 1D CNF in cell walls which could effectively contact with the adjacent nanoparticles and hence formed a relatively stable conductive network in cell walls. As for foam samples of 1D/2D 1:1, 1D/2D 1:2 and 2D (only GNP), the conductivity decreased significantly after $scCO_2$ foaming, which implies the destruction of conductive network due to the disconnected nanoparticles in cell walls. By summarizing the conductivity changes of all samples before and after $scCO_2$ foaming, it can be speculated that a transition occurs at the foam sample of 1D/2D 2:1. More 1D CNF (1D and 1D/2D 4:1) leads to more stable conductive network even after $scCO_2$ foaming, but more 2D GNP (1D/2D 1:1, 1D/2D 1:2 and 2D) leads to less stable conductive network after $scCO_2$ foaming. Therefore, 1D/2D 2:1 sample foamed at 155°C falls into the percolation 1D/2D proportion which would exhibit a high sensitive response by the construction and/or destruction of conductive network in cell walls.

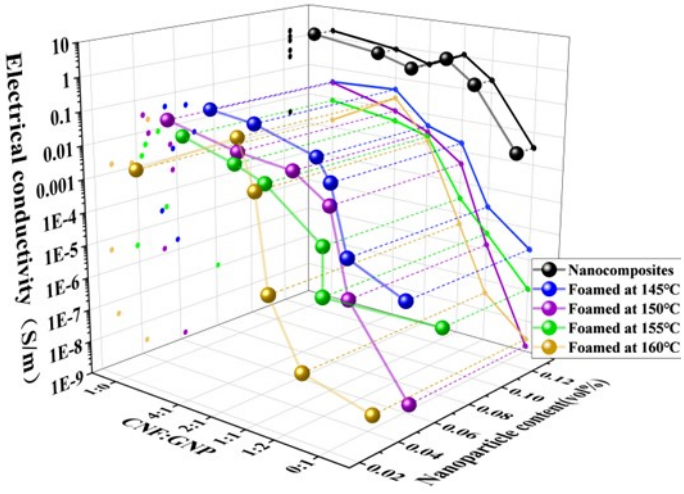

Figure S5 Electrical conductivity of solid nanocomposites and the corresponding foams at various foaming temperature

Nanocomposite foams with different 1D CNF/2D GNP ratio and prepared at different foaming temperature were tested to analyze their strain sensing performance, including electrical resistance and $\Delta R/R_0$, as shown in Figure S6. It is noted that the nanocomposite foams prepared at relatively low foaming temperature had low expansion ratio. The conductive path in the unfoamed nanocomposite was then less affected by foaming and could still maintain a relatively stable structure during stretching. Therefore, the sensing response was weak. However, if foaming temperature was too high resulting in a too large expansion ratio (like 4 folds), the conductive path was destroyed by foaming, and hence failed to generate any resistance signal during stretching. Therefore, a proper foaming temperature like 155℃ is very important to regulate the conductive path in a percolation status so as to achieve high sensing performance.

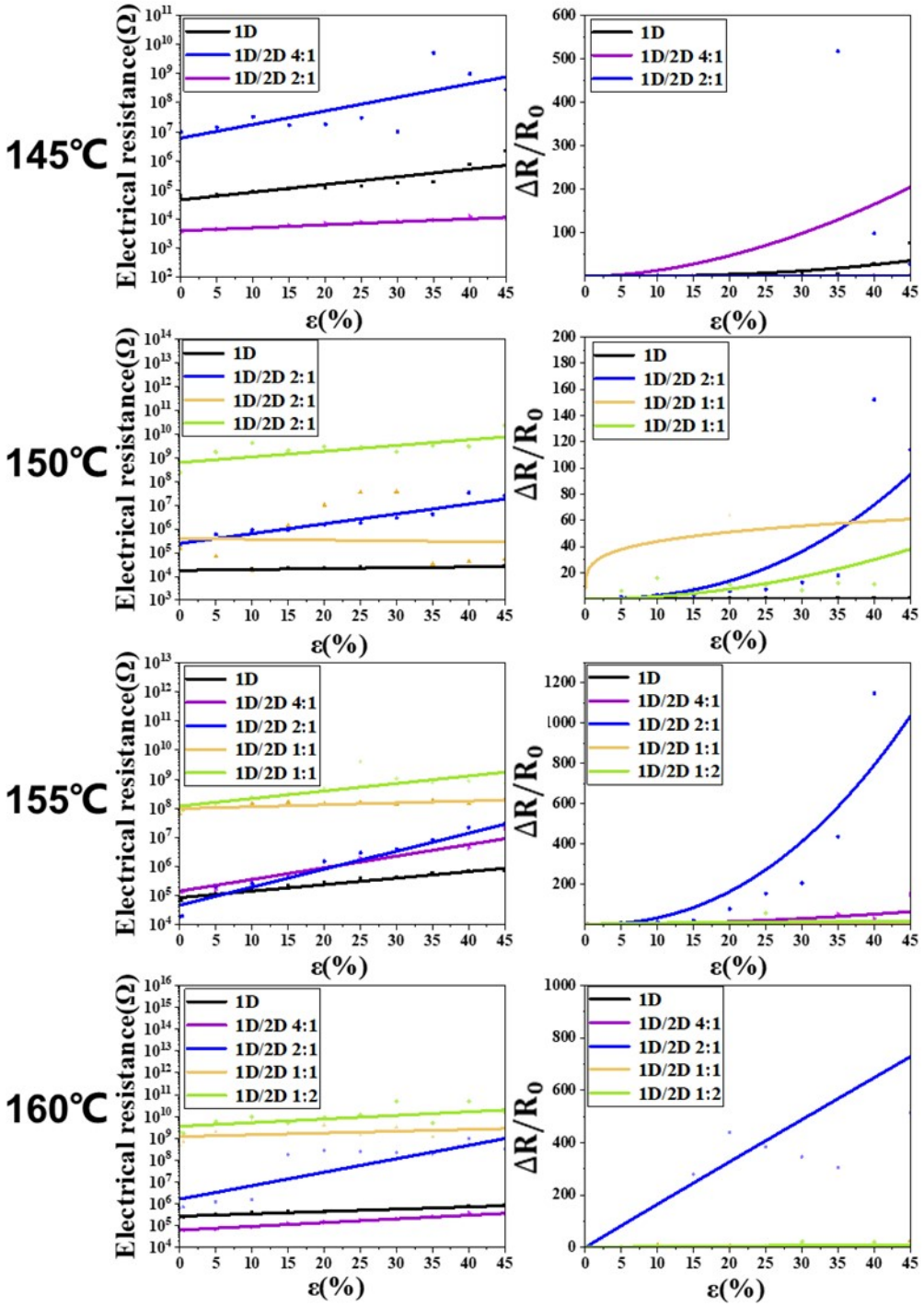

Figure S6 Strain sensing performance of nanocomposite foams with different CNF/GNP ratio prepared at various foaming temperatures of 145℃, 150℃, 155℃ and 160℃: electrical resistance and $\Delta R/R_0$ *vs* strain

As shown in Figure S7 (a), an increased nanoparticle content inhibits cell growth and reduces the expansion ratio, which is not conducive to the nanoparticle distribution;

a decreased nanoparticle content makes the cell wall smoother and the corresponding assembled sensor softer. In Figure S7 (b), 5 wt% and 10 wt% nanoparticle content have too high initial electrical resistance due to the relatively low content of conductive nanoparticles, especially samples with 5 wt% nanoparticle content, which cannot even be stably detected because of the too high electrical resistance. This corresponds to a larger average shortest distance in the model. The samples with 20 wt% nanoparticle exhibited a smaller average shortest distance in the model and hence a higher initial conductivity. The experimental results are consistent with the expectation, but such sample with 20 wt% nanoparticle is difficult to achieve high stretching ratio (like more than 42%). It shows that the model can be used to speculate experimental results especially for cases which are difficult to achieve experimentally.

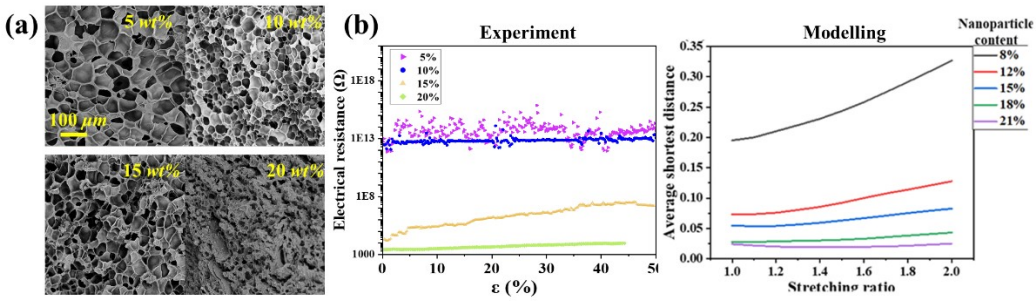

Figure S7 (a) the cell morphology at different nanoparticle content; (b)the resistance changes during stretching process and simulation result with different nanoparticle content.

In Figure S8, the foam sample has been tested for at least hundreds of stretching cycles and then was fractured at different modes for SEM observation: (a) cutting with scissors; (b) cryogenic breaking in liquid nitrogen; and (c) tensile breaking under a huge external force at very large tensile strain. It can be seen from Figure S8 that nanoparticles were still well dispersed in cell walls, and no obvious cracks were observed in cell walls. Especially for tensile breaking as shown in Figure S8 (c), although nanoparticles were obviously extracted from TPU after tensile fracture process, the surface morphology of the cell wall is basically consistent with its original morphology (before tensile breaking). Therefore, we think that the main factor of the formation of conductive network is not the cracks, but the overlap between the

conductive nanoparticles inside it.

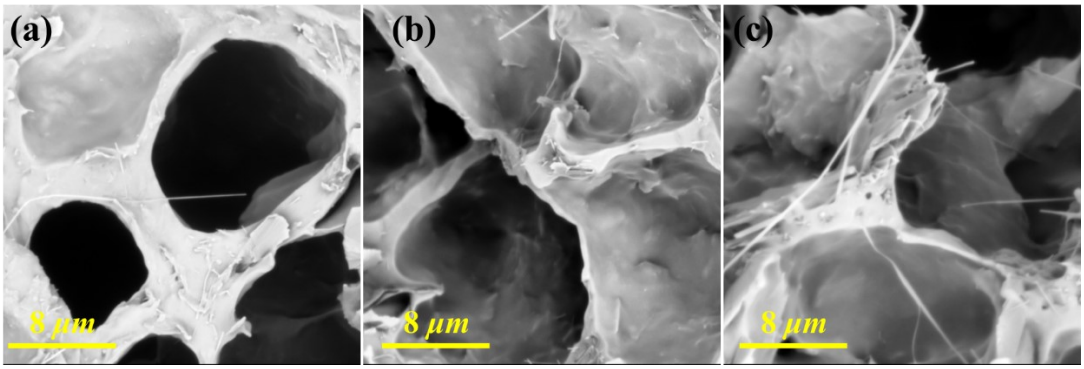

Figure S8 Cell wall morphology of foam sample under different fracture modes: (a) cutting with scissors; (b) cryogenic breaking in liquid nitrogen; and (c) tensile breaking under a huge external force

The mechanical properties of the nanocomposites before and after foaming are shown in Figure S9. Due to introduction of air phase in nanocomposite, the mechanical strength of foam became much lower than that of the solid nanocomposite. However, foaming has little effect on tensile strain, which is beneficial to fabricate flexible strain sensor; because foaming could effectively enhance the sensing performance and meanwhile could effectively decrease the tensile stress.

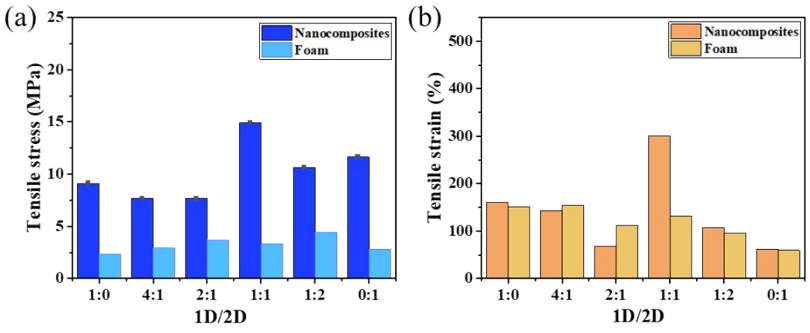

Figure S9 Mechanical properties of nanocomposites and corresponding foams: (a) tensile stress; (b) tensile strain

The relationship between the thermal conductivity and the nanoparticle proportion is shown in Figure S10. It is noted that nanoparticles significantly improved the thermal

conductivity, the higher 2D GNP proportion, the larger thermal conductivity. However, the introduction of a large amount of air after foaming significantly decreased the thermal conductivity of the foams due to the very low thermal conductivity of air phase. Therefore, the flexible strain sensor made from nanocomposite foam has the characteristics of light weight, good flexibility and heat insulation performance.

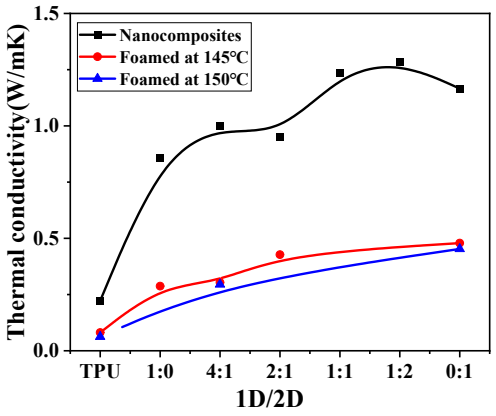

Figure S10 Thermal conductivity of pristine TPU, nanocomposites and corresponding foams with 15 wt% hybrid 1D/2D nanoparticle